

PCCP

Accepted Manuscript

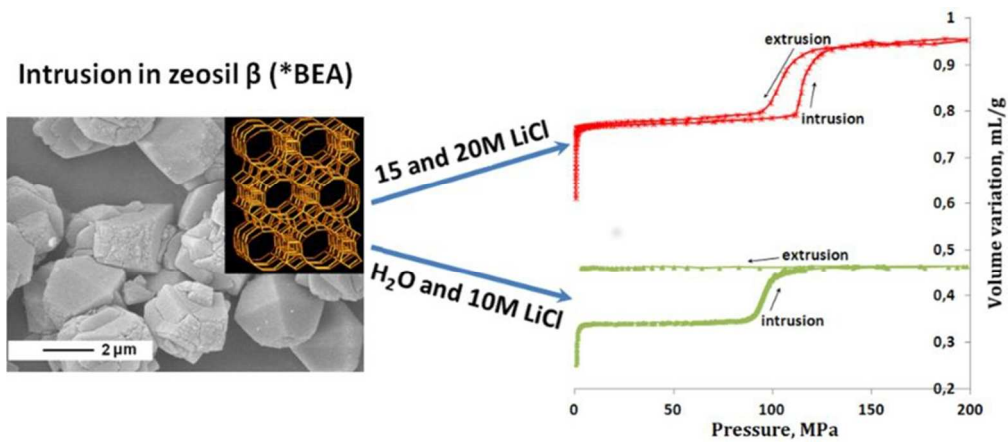


This is an *Accepted Manuscript*, which has been through the Royal Society of Chemistry peer review process and has been accepted for publication.

Accepted Manuscripts are published online shortly after acceptance, before technical editing, formatting and proof reading. Using this free service, authors can make their results available to the community, in citable form, before we publish the edited article. We will replace this *Accepted Manuscript* with the edited and formatted *Advance Article* as soon as it is available.

You can find more information about *Accepted Manuscripts* in the [Information for Authors](#).

Please note that technical editing may introduce minor changes to the text and/or graphics, which may alter content. The journal's standard [Terms & Conditions](#) and the [Ethical guidelines](#) still apply. In no event shall the Royal Society of Chemistry be held responsible for any errors or omissions in this *Accepted Manuscript* or any consequences arising from the use of any information it contains.



A behavior of high pressure intrusion-extrusion of electrolyte solutions in pure silica*BEA-type zeolite depends drastically on electrolyte concentration.
79x35mm (300 x 299 DPI)

Drastic change of the intrusion-extrusion behavior of electrolyte solutions in pure silica*BEA-type zeolite

Cite this: DOI: 10.1039/x0xx00000x

A. Ryzhikov*, I. Khay, H. Nouali, T.J. Daou, J. Patarin*

Received 00th January 2012,
Accepted 00th January 2012

DOI: 10.1039/x0xx00000x

www.rsc.org/

High pressure water and electrolyte solutions intrusion-extrusion experiments in pure-silica *BEA-type zeolite (zeosil β) were performed in order to study the performances of these systems in energy absorption and storage. The "zeosil β -water" system displays a bumper behavior with an intrusion pressure of 53 MPa and an absorbed energy of 8.3 J/g. For the "zeosil β -LiCl aqueous solutions" systems the intrusion pressure increases with the LiCl concentration to 95, 111 and 115 MPa for 10, 15 and 20 M solution, respectively. However, for concentrations above 10M, a transformation of the system behavior from bumper to shock-absorber is observed. The zeolite samples were characterized by several structural and physicochemical methods (XRD, TGA, solid-state NMR, N_2 physisorption, ICP-OES) before and after intrusion-extrusion experiments in order to understand the influence of the LiCl concentration on the intrusion-extrusion behavior. It is shown that the intrusion of water and LiCl solutions with low concentration leads to the formation of Si-(OSi) $_3$ OH groups, whereas no defects are observed under intrusion of concentrated LiCl solutions. A possible mechanism of LiCl solution intrusion based on separate intrusion of H $_2$ O molecules and Li(H $_2$ O) $_x^+$ ions is proposed.

Introduction

Zeolites are microporous solids with a framework built from TO $_4$ tetrahedra (T=Si,Al) which form cages, channels and cavities. They are widely used in industrial catalysis, adsorption, molecular sieving and ion-exchange processes.¹ Since our pioneering work^{2,3} several pure-silica zeolites (zeosils) were studied for potential applications in energy storage or absorption.⁴⁻¹⁶ This approach is based on high pressure intrusion of liquid water into the pores of zeosils, which are known to have hydrophobic properties. Under intrusion liquid water is transformed into a multitude of molecular clusters in the pores. Thus, the supplied mechanical energy during the compression step is converted to interfacial energy. By reducing the pressure, the system can induce an expulsion of the liquid out of the pores of zeolite (extrusion). Depending on zeolite structure, the "zeosil-water" system is able to restore, dissipate, or absorb energy and therefore, it displays a spring, shock-absorber, or bumper behavior. A summary of energetic performances of pure-silica zeolites with different crystalline structures was previously reported.¹⁶ Most of the studied "zeosil-water" systems display a spring behavior, however some of them show a shock-absorber (RRO)¹¹ or bumper (*BEA², IFR¹⁰) behavior. The *BEA-type zeolite is characterized by a three-dimensional channel system with 12-membered ring (MR) openings (0.56 and 0.66-0.77 nm). It is a disordered structure which consists of two distinct polytypes and the non reversibility of the phenomenon (bumper behavior) was explained by the presence of hydrophilic silanol defects at the interface of the polytypes which interact with water molecules⁴. The intrusion-extrusion of different electrolyte solutions in hydrophobic porous solids was studied recently in order to improve

their energetic performances.^{17,18} It was found that highly concentrated aqueous solutions of salts such as LiCl, NaCl, MgCl $_2$ enhanced the intrusion pressure up to 3 times (in the case of the "Silicalite-1-LiCl 20M" system).¹⁸ Similarly, an increase of energetic performances was observed in high-silica faujasite and ZSM-5 zeolites.¹⁹⁻²⁰ In the work of Han et al.²¹ the intrusion of NaCl and NaBr solution in high silica FAU-type zeolites was found to increase considerably the intrusion pressure and a shock-absorber behavior was observed for the corresponding systems. The influence of LiCl concentration was studied recently in our team for "Silicalite-1-LiCl aqueous solutions" systems.²² It was found that the intrusion pressure grows homogeneously with the LiCl concentration without any change of the system behavior. The increase of the intrusion pressure with the electrolyte concentration was explained by a higher solid-liquid interfacial tension and/or by the ions desolvation phenomenon.²²

In this paper, the influence of the LiCl electrolyte concentration on the high-pressure behavior of "*BEA-type zeosil-electrolyte solutions" systems with a thorough characterization by multiple structural and physicochemical methods is reported.

Results and discussion

Intrusion-Extrusion Isotherms. The pressure-volume diagrams of the "zeosil β -water" and the "zeosil β -LiCl aqueous solutions" systems are shown in Figure 1. The corresponding data are reported in Table 1. Three intrusion-extrusion cycles were performed for each experiment. Only the first cycle of all the experiments is presented in Figure 1. As it was shown in previous works, the volume variation observed at low pressure (< 1 MPa) corresponds to the compression

and the liquid filling in the interparticular porosity of the zeolitic pellet.^{14,15} In the case of the “zeosil β -water” system an irreversible intrusion is observed in the 1st cycle at the pressure of 53 MPa. From the NMR results described below (see NMR section), this bumper behavior is rather related to the formation of hydrophilic silanol defects during the intrusion step than their presence in the nonintruded sample (see introduction). These defects interact with the intruded water molecules and therefore no extrusion is observed. A similar behavior is also noticed for the “zeosil β - LiCl aqueous solutions” systems with concentration of 10 M. However, the intrusion pressure increases up to 95 MPa. Such an increase can be explained by a higher solid-liquid interfacial tension, according to the Laplace-Washburn equation ($P_L = (2\sigma \cos\theta/r)$, where σ is the surface tension, r the pore radius and θ the contact angle between solid and the liquid), but the variation of the surface tension for concentrated LiCl aqueous solutions (about 25%)²³ is considerably lower than the observed intrusion pressure increase (79% for 10M LiCl). Another ways to explain the pressure increase could be the ions desolvation phenomenon¹⁸ or confinement effect of nanopore walls.^{19,21}

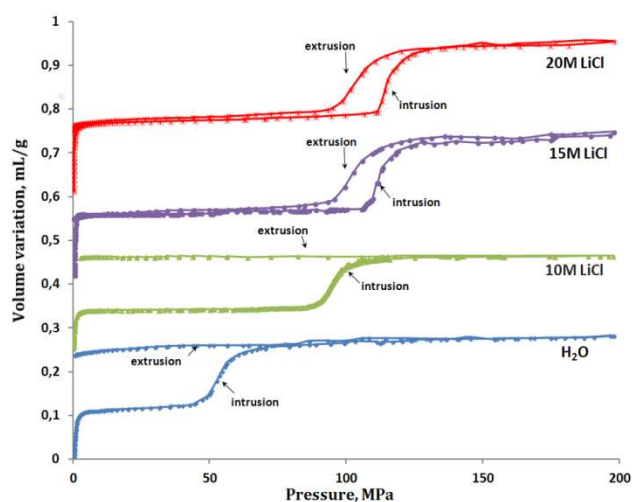


Figure 1. The first intrusion-extrusion cycle of the “zeosil β -water” and the different “zeosil β -LiCl aqueous solution” systems. For a better visibility, the diagrams are shifted along the Y-axis.

Table 1. Characteristics of the “zeosil β - solutions” systems: intrusion (P_{int}) and extrusion (P_{ext}) pressures, intruded (V_{int}) and extruded (V_{ext}) volumes, stored (E_s) and restored (E_r) energies and the energy yield.

| | Zeosil β - Water | Zeosil β - 10M LiCl | Zeosil β - 15M LiCl | Zeosil β - 20M LiCl |
|--------------------|------------------------|---------------------------|---------------------------|---------------------------|
| P_{int}^a (MPa) | 53 | 95 | 111 | 115 |
| V_{int}^a (mL/g) | 0.14 | 0.12 | 0.16 | 0.16 |
| P_{ext}^a (MPa) | - | - | 102 | 103 |
| V_{ext}^a (mL/g) | - | - | 0.16 | 0.16 |
| E_s^b (J/g) | 8.3* | 11.4* | 17.8 | 18.4 |
| E_r^c (J/g) | - | - | 16.3 | 16.5 |
| Yield (%) | - | - | 91 | 90 |
| Behavior | bumper | bumper | shock-absorber | shock-absorber |

(a) determined from intrusion-extrusion isotherms

(b) stored energy $E_s = V_{int} \times P_{int}$

(c) restored energy $E_r = V_{ext} \times P_{ext}$

* Absorbed energy (no extrusion)

The following increase of the LiCl aqueous concentration above 10 M leads to a drastic change of the system behavior. “Zeosil β -15 M and 20 M LiCl solutions” systems show a shock-absorber behavior. A slight hysteresis between the intrusion and extrusion curves, which is a little more pronounced for the 20 M LiCl solution, is observed. The energy yield is about 90-91 %. The system is reproducible over several cycles. The intrusion pressures are close to 111 and 115 MPa for 15 and 20 M LiCl solutions, respectively and the extrusion pressures to 102 and 103 MPa.

To our knowledge, such a change of behavior from bumper to shock-absorber was never reported previously and merits to be thoroughly studied.

XRD and SEM Characterizations. The XRD patterns of the zeosil β samples before and after intrusion-extrusion of water and 20 M LiCl aqueous solution are given in Figure 2. The patterns show sequence of large and narrow diffraction peaks typical for the *BEA disordered structure. A shift of the XRD peaks to higher angle values is observed after intrusion-extrusion experiments, which corresponds to a contraction of the crystalline lattice. The XRD patterns were indexed in the tetragonal symmetry (space group $P4_122$). The corresponding unit-cell parameters are reported in Table 2. A slight decrease of the unit-cell volume (from 4070 to 3973 \AA^3) is observed after water and 20 M LiCl intrusion-extrusion experiments. As already reported for the ITW-type zeosil¹⁵ the creation of defect sites under high pressure might be responsible of this change.

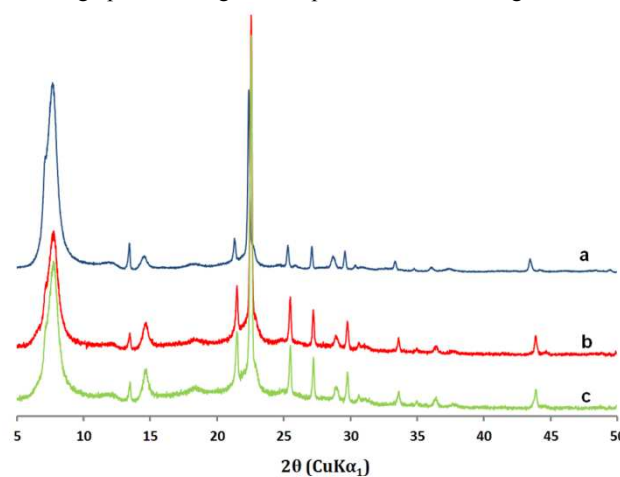


Figure 2. X-ray diffraction patterns of zeosil β samples before (a) and after three intrusion-extrusion cycles in (b) water and (c) 20 M LiCl aqueous solution.

The crystal morphology of the zeosil β samples was examined by scanning electron microscopy. For the nonintruded sample, truncated square bipyramidal crystals with sizes of 2-4 μm are observed (Figure 3a). They are not single crystals because the tops of pyramids show irregularities corresponding to the stacking of small crystallites. After the intrusion-extrusion experiments the crystals are partially broken, in particular, in the case of LiCl solution (Figures 3b and 3c).

Table 2. Unit-cell parameters of zeosil β samples before and after three intrusion-extrusion cycles in water and 20 M LiCl aqueous solution.

| Sample | a (\AA) | c (\AA) | V (\AA^3) |
|---------------------------|--------------------|--------------------|----------------------|
| Zeosil β | 12.456(4) | 26.229(9) | 4069.8(30) |
| Zeosil β (water) | 12.348(6) | 26.109(13) | 3980.7(45) |
| Zeosil β (20M LiCl) | 12.339(4) | 26.097(10) | 3973.2(25) |

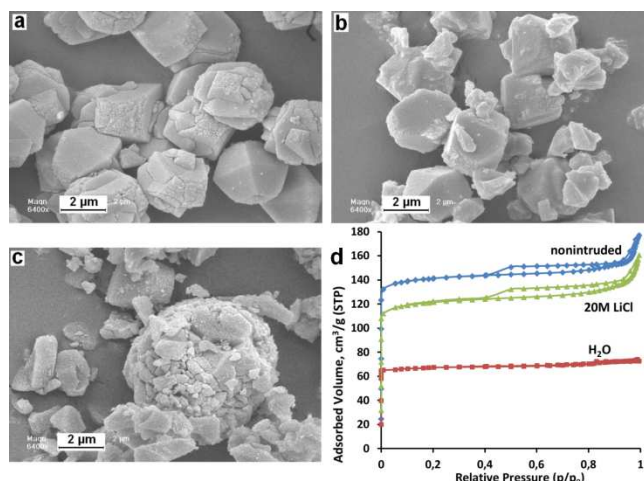


Figure 3. SEM micrographs of the zeosil β samples before (a) and after three intrusion-extrusion cycles in (b) water, (c) in 20M LiCl aqueous solution, (d) N_2 adsorption-desorption isotherms at $-196\text{ }^\circ\text{C}$ of the zeosil β samples before and after three intrusion-extrusion cycles in water and 20 M LiCl aqueous solution.

N_2 Adsorption-Desorption Isotherms. The N_2 adsorption-desorption isotherms of the nonintruded and some intruded samples are shown in Figure 3d. The isotherms are mainly of type I characteristic of microporous solids. The BET surface area and microporous volume of the nonintruded sample is equal to $596\text{ m}^2/\text{g}$ and $0.21\text{ cm}^3/\text{g}$. For the intruded-extruded sample with water and 10 M LiCl solution (not reported), the surface area and pore volume are considerably lower: $S_{\text{BET}} = 275$ and $335\text{ m}^2/\text{g}^{-1}$ and $V_{\text{micro}} = 0.10$ and $0.13\text{ cm}^3/\text{g}^{-1}$, respectively, revealing thus, in agreement with the TG and NMR results (see below), the creation of defect sites in these samples and the presence of nonexpelled water in the porosity. It is not the case for the samples intruded with concentrated LiCl solutions, the surface area is only a little lower than for the nonintruded one: 498 and $480\text{ m}^2/\text{g}^{-1}$ for 15 and 20 M LiCl solutions, respectively, with, in both cases, a pore volume of $0.18\text{ cm}^3/\text{g}^{-1}$. As it will be seen below, no defect or only few defects are present in these samples.

Thermal Analysis. The experimental results issued from the thermogravimetric (TG) analysis of the zeosil β samples before and after intrusion-extrusion experiments are depicted in Figure 4. The total weight loss of the nonintruded sample is quite low (1.07 %), confirming the hydrophobic character of the pure silica *BEA-type zeolite. Thermogravimetric curves of the samples after intrusion of water and 10 M LiCl are completely different. The total weight loss close to 14.9 and 11.9 %, respectively occurs in three main steps. The first one (5.8-6.2 %), located between 30 and $160\text{ }^\circ\text{C}$, is ascribed to the desorption of physisorbed water molecules. In the case of the 10 M LiCl intruded sample, the second step of 3.0 % is located at $160\text{-}290\text{ }^\circ\text{C}$, and the third one of 2.7 % at higher temperature ($300\text{-}500\text{ }^\circ\text{C}$). For the water-intruded sample these steps overlap and are more strained. The second step begins at $230\text{ }^\circ\text{C}$ and the third one at $\sim 350\text{ }^\circ\text{C}$ with a total weight loss for both steps of 9.1 %. It can be supposed that the second step corresponds to the removal of water molecules adsorbed on silanol groups, and the third one to the removal of water molecules arising from dehydroxylation reactions. This loss corresponds to 13 OH-groups per unit cell ($\text{Si}_{64}\text{O}_{128}$) for the 10 M LiCl intruded-extruded sample and to ~ 18 OH-groups per unit cell in the case of the water intruded-extruded sample. Surprisingly, the samples after intrusion-extrusion experiments with highly concentrated LiCl solutions demonstrate low total weight loss

similar to that of the nonintruded sample: 1.2 % and 1.5 % for 20 and 15 M solutions, respectively. The weight losses occur in two badly pronounced steps. The first one (0.6 to 0.8 wt %), located between 30 and $250\text{ }^\circ\text{C}$, corresponds to the desorption of physisorbed water molecules. The second strained weight loss, in the temperature range of $250\text{-}800\text{ }^\circ\text{C}$, can be assigned mainly to water arising from dehydroxylation reactions. This loss corresponds to about 2 OH groups per unit cell ($\text{Si}_{64}\text{O}_{128}$) for the nonintruded sample and 2.5 and 3.0 OH groups for the intruded-extruded samples with 20 and 15 M LiCl solutions, respectively. It can be concluded that the intrusion of water and LiCl solutions with low concentration leads to the breaking of siloxane bridges and consequently to the formation of a higher number of silanol groups; while highly concentrated LiCl (15 and 20 M) solutions do not form such silanol defects. Thus, there is a correlation between the change of intrusion-extrusion behavior and the thermogravimetric experiments.

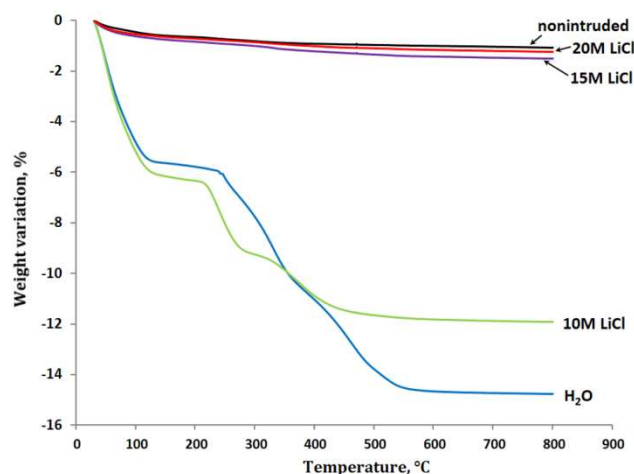


Figure 4. TG curves of the zeosil β samples before and after three intrusion-extrusion cycles in water, 10 M, 15 M and 20 M LiCl aqueous solutions.

^{29}Si MAS NMR Spectroscopy. The ^{29}Si MAS NMR spectra of the zeosil β samples before and after intrusion-extrusion experiments with water, 10 M, 15 M and 20 M LiCl solutions are shown in Figure 5. The spectrum of the nonintruded sample exhibits 3 main resonances in the -109 to -115 ppm range ascribed to the non equivalent crystallographic silicon Q_4 sites. No signals assigned to Q_3 groups corresponding to defects such as Si-OH groups and expected at about -100 ppm are observed. After water and 10 M LiCl solutions intrusion-extrusion experiments the spectra change considerably. Two new resonances at -101.5 and -105 ppm appear. They are characteristic of Q_3 sites and reveal the formation of silanol (Si-(OSi) $_3$ OH) groups. A significant loss of resolution is also observed, illustrated by the broadening of all Q_4 sites, which might indicate modifications of bond angles and a decrease of the local structural order of the inorganic framework. The existence of Q_3 sites which represent about 14 % of the total Si is in agreement with TG data. After intrusion-extrusion experiments with 15 and 20 M LiCl solutions the spectra are almost the same than the one for the nonintruded sample which confirms the absence of silanol formation under intrusion of highly concentrated LiCl solutions in agreement with the TG and N_2 -adsorption-desorption results described above.

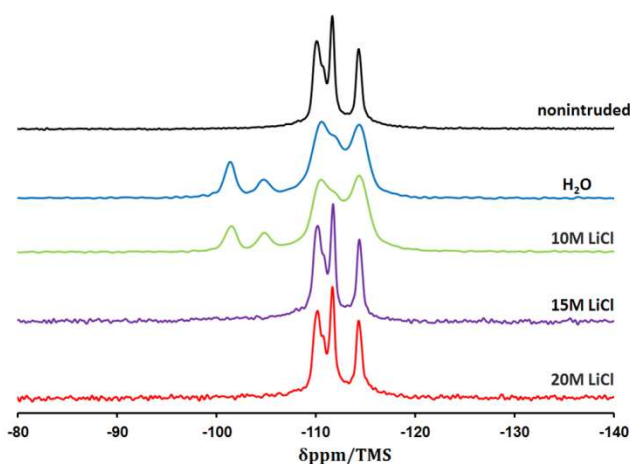


Figure 5. ^{29}Si -MAS NMR spectra of the zeosil β samples before and after three intrusion-extrusion cycles in water, 10 M, 15 M and 20 M LiCl aqueous solutions.

^1H - ^{29}Si CPMAS NMR Spectroscopy. The ^1H - ^{29}Si CPMAS NMR spectra of the non-intruded sample and the samples intruded with water, 10 M, 15 M and 20 M LiCl are reported in Figure 6. These spectra were performed in order to enhance the silicon atoms that bear protons and thus to get evidence of the presence of silanol groups. As expected, under these NMR experimental conditions (short contact time), the spectra of the nonintruded and intruded samples with 15 and 20 M LiCl solutions provide a weak signal indicating that only very few defect sites are present. After intrusion-extrusion of water and 10 M LiCl solution under the same experimental conditions, the signal to noise ratio of both spectra is considerably higher and two resonances at -101.5 and -105 ppm corresponding to Q_3 sites appear clearly. No significant difference is observed for the ^1H - ^{29}Si CPMAS spectra of water and 10 M LiCl-intruded samples.

^1H -MAS NMR. The ^1H -MAS NMR spectra of the nonintruded and intruded samples (water, 10 M, 15 M and 20 M LiCl) are shown in Figure 7. The ^1H -MAS NMR allows to characterize the hydrogenated species in silicates. In the case of the nonintruded sample a main resonance is observed at 3.3 ppm with an additional small resonance at 4.6 ppm (not visible on Figure 7). They are characteristic to water adsorbed molecules. However, the intensity of the corresponding components is very low, indicating that the defect sites are few and consequently this sample is hydrophobic. The same low intensity of the ^1H -MAS NMR signal is also observed for the 15 M and 20 M LiCl intruded-extruded samples, which is in correlation with the TG and ^{29}Si NMR results. For the sample intruded with 15 M LiCl solutions a main resonance at 4.2 ppm with a shoulder at 3.3 ppm assigned to adsorbed water is observed. Another small resonance at 0.8 ppm can be ascribed to the protons of silanol groups. In the case of 20 M LiCl intruded-extruded sample, the spectrum is similar, but the main resonance is observed at 3.7 ppm and there are two small resonances at 1.1 and 0 ppm. The spectrum of water-intruded sample is completely different. Three resonances of high intensity are observed at 4.0, 1.2 and 0.8 ppm. The first one can be assigned to adsorbed water molecules, the others – to silanol groups ($=\text{Si}-\text{OH}$).²⁴ In the case of the sample intruded with 10 M LiCl a resonance of high intensity at 3.7 ppm is observed. Surprisingly the intensity of two resonances corresponding to silanol groups (1.0 ppm and 0 ppm) is very low, whereas highly intensive resonances of silanol groups are clearly observed on the CP-MAS spectrum.

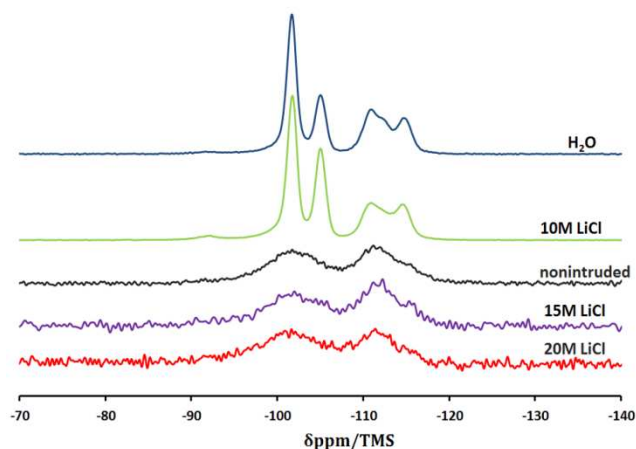


Figure 6. ^1H - ^{29}Si CPMAS NMR spectra of the zeosil β samples before and after three intrusion-extrusion cycles in water, 10 M, 15 M and 20 M LiCl aqueous solutions.

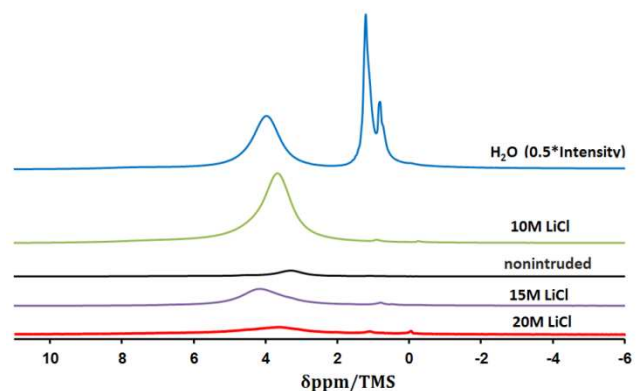


Figure 7. ^1H -MAS NMR spectra of the zeosil β samples before and after three intrusion-extrusion cycles in water, 10 M, 15 M and 20 M LiCl aqueous solutions.

ICP/OES Analysis. In order to get or not evidence of the presence of lithium ions into the micropore volume of the solids after intrusion-extrusion experiments, ICP/OES analyses were performed. The intruded-extruded samples with 10, 15 and 20 M LiCl after washing in deionized water contains about 0.01 wt % of lithium, corresponding to about 0.07 lithium atom per unit cell (64 Si). Thus, it can be concluded that whatever the LiCl concentration, no lithium cations are present in the intruded-extruded samples. That means, for the intruded-extruded sample with 10M LiCl solutions for which a bumper behavior is observed, that only water molecules penetrate into the pores of the zeosil β . According to the TG and NMR results, these molecules contribute to the breaking of siloxane bridges leading to the formation of $\text{Si}-(\text{OSi})_3\text{OH}$ groups.

The change of the system behavior for LiCl concentrations of 15 M and above might be explained by a change of the nature of the intruded liquid. For these samples, the intruded liquid is nonwetting and does not lead to the formation of defect sites (see NMR and TG results). Therefore, we can conclude that the intruded liquid is not free water molecules otherwise, as observed and described above for the “zeosil β -water or LiCl 10M solution” system, silanol defects would have been created. Generally, it is considered that lithium ion is present in the aqueous solutions in the form of $\text{Li}(\text{H}_2\text{O})_4^+$ ions^{25,26}, the chlorine ion is hydrated by about 6 water molecules²⁷, however the energy of chlorine-hydrate bonds is considerably lower than the

one for hydrated lithium^{28,29}. Thus, it can be supposed that the solvation of lithium ion should be predominant. The concentration of 15 M corresponds to the ratio 1 LiCl : 3.75 H₂O. It can be assumed that at LiCl concentrations higher than 15M, all the water molecules are strongly bonded to lithium ions (solvated species Li(H₂O)_x⁺) which are intruded with Cl⁻ ions in the porosity without affected the zeolite framework (absence of defect sites). At lower LiCl concentration (10M solution corresponds to the ratio 1 LiCl : 5.6 H₂O) there are some water molecules which are not strongly bounded with lithium ions, and under pressure these water molecules are intruded into the pores.

Taking as a basis the model of separate intrusion of H₂O and hydrated ions, it can be supposed that an increase of intrusion pressure between pure water (53 MPa) and 10M LiCl solution (95 MPa) is related essentially to the desolvation of water molecules from hydrated anions and cations. The following increase of intrusion pressure at higher concentration (15 and 20 M) is related to the change of intruded species – from free water to Li(H₂O)_x⁺ and Cl⁻ ions.

Experimental

*BEA-type zeolite was synthesized in fluoride medium according to a procedure similar to that described in reference.³⁰ The synthesis requires the presence of tetraethylammonium (TEA) cations as structure-directing agents (40% solution of tetraethylammonium hydroxide (TEAOH), Aldrich). Tetraethoxysilane (TEOS, Aldrich, 98%) was used as the silica source. The reaction gel had the following molar composition: 1 SiO₂ : 0.7 TEAOH : 0.7 HF (40%, Normapur) : 10 H₂O. The mixture, transferred into a PTFE-lined stainless-steel autoclave, was heated at 150 °C for 6 days. After synthesis, the solid was calcined under air at 600 °C during 5 hours in order to remove the organic template. The intrusion–extrusion experiments of aqueous solutions in the zeosil sample in the form of compressed pellets were performed at room temperature using a modified mercury porosimeter (Micromeritics Model Autopore IV), as described in our previous works.²² Before these experiments, the pellets were outgassed at 300 °C under vacuum. The liquid phase was either pure water or aqueous solution of lithium chloride at concentration of 10, 15 or 20 M. The compressibility of pure water or LiCl aqueous solution was subtracted from the experimental intrusion–extrusion curves. The values of the intrusion (P_{int}) and extrusion (P_{ext}) pressures correspond to that of the half volume total variation. The pressure is expressed in megapascals (MPa) and the volume variation in milliliters (mL) per gram of outgassed samples. The experimental error is estimated to 1 % on the pressure and on the volume.

After intrusion–extrusion experiments, the samples intruded with LiCl were washed with water to remove traces of LiCl for the following analyses. The absence of chloride anions in the filtrate was controlled by adding few drops of 1 M silver nitrate aqueous solution (no silver chloride precipitate). Then the samples were dried at 70 °C overnight, and hydrated in 80 % relative humidity atmosphere during 24 h in order to set the hydration state.

X-ray diffraction patterns of the different samples were recorded in a Debye–Scherrer geometry on a STOE STADI-P diffractometer equipped with a curved germanium (111), primary monochromator, and a linear position-sensitive detector (6° 2θ) using Cu Kα₁ radiation (λ = 0.15406 nm). Measurements were achieved for 2θ angle values in the 3–50 range, step 0.15° 2θ, and time/step = 120 s. The unit-cell parameters were determined using Louër's DICVOL91 indexing routine³¹ of the STOE WinXPOW program package.³²

The size and the morphology of the crystals were determined by scanning electron microscopy (SEM) using a Philips XL 30 FEG microscope.

Nitrogen adsorption–desorption isotherms were performed at -196 °C using a Micromeritics ASAP 2420 apparatus. Prior to the adsorption measurements, the samples were outgassed at 90°C overnight under vacuum to eliminate physisorbed water. Low degassing temperature was chosen to avoid the dehydroxylation process. The specific surface area (S_{BET}) and microporous volume (V_{micro}) were calculated using the BET and t-plot methods, respectively.

Thermogravimetric (TG) analyses were carried out on a TG Mettler Toledo STARE apparatus, under air flow, with a heating rate of 5 °C/min from 30 to 800 °C.

Measurements by Inductively Coupled Plasma Optical Emission Spectroscopy (ICP-OES) were carried out using a Thermo Model 6300DUO spectrometer in order to determine the presence of lithium atoms into the pores of zeolite after intrusion–extrusion experiments. The lithium concentration was determined after digestion of samples in HF, neutralization by H₃BO₃, filtration and dilution up to 50 mL with ultra-pure water. The wavelength of the corresponding spectrometric lines that were used for the analysis was Li: 670.784 nm.

¹H MAS, ²⁹Si MAS and ¹H–²⁹Si CPMAS NMR spectra were recorded on a Bruker Advance II 300 MHz spectrometer, with a double-channel 7 mm Bruker MAS probe. The recording conditions are given in Table 3.

Table 3. Recording Conditions of the ¹H MAS, ²⁹Si MAS and ¹H–²⁹Si CPMAS NMR Spectra.

| | ¹ H | ²⁹ Si | |
|-------------------------|------------------|------------------|------------------|
| | MAS | MAS | CP MAS |
| Chemical shift standard | TMS ^a | TMS ^a | TMS ^a |
| Frequency (MHz) | 300.07 | 59.6 | 59.6 |
| Pulse width (μs) | 5.06 | 1.87 | 4 |
| Flip angle | π/2 | π/6 | π/2 |
| Contact time (ms) | / | / | 8 |
| Recycle time (s) | 10 ^b | 80 | 10 ^b |
| Spinning rate (kHz) | 4 | 4 | 4 |
| Scans number | 8 | 1000 | 16000 |

^a TMS : TetraMethylSilane

^b The relaxation time t₁ was optimized

Conclusions

The influence of the concentration on intrusion–extrusion of LiCl aqueous solution in pure-silica *BEA-type zeolite (zeosil β) has been studied. It was revealed that the “zeosil β–LiCl aqueous solutions” systems show a bumper behavior for LiCl concentration equal or below 10 M. The intrusion pressure increases with electrolyte concentration from 53 MPa for pure water to 95 MPa for 10 M LiCl solution and the absorbed energy from 8.3 to 11.4 J/g. The “Zeosil β–LiCl aqueous solutions” systems with concentration equal or higher than 15 M display a shock-absorber behavior with an intrusion pressure of 111 and 115 MPa for 15 and 20 M LiCl, respectively and in both cases, a stored energy of 16.5 J/g. To our knowledge, such a change of the system behavior was never observed previously. The transformation of the system behavior from bumper to shock-absorber can be explained by the separate penetration of free water molecules and solvated ions in the zeolite porosity. At low LiCl concentrations, free water molecules are intruded. They contribute to

a breaking of siloxane bridges with the formation of silanol defects. For LiCl concentrations of 15 M and above, water molecules are bonded to lithium ions (solvated $\text{Li}(\text{H}_2\text{O})_x^+$ ions) and are intruded in the porosity without affected the zeolite framework. Indeed, solid-state NMR and TGA measurements confirm the absence of hydroxyl groups after intrusion of concentrated LiCl solutions.

Acknowledgements

The authors would like to thank Dr. S. Rigolet for fruitful discussions.

Notes and references

Université de Haute Alsace (UHA), CNRS, Equipe Matériaux à Porosité Contrôlée (MPC), Institut de Science des Matériaux de Mulhouse (IS2M), UMR 7361, ENSCMu, 3 bis rue Alfred Werner, F-68093 Mulhouse, France.
E-mail: andrey.ryzhikov@uha.fr; joel.patarin@uha.fr

- 1 J. Čejka, H. Van Bekkum, A. Corma and F. Schüth, *Stud. Surf. Sci. Catal.*, 2007, **168**, 525.
- 2 V. Eroshenko, R. C. Regis, M. Soulard and J. Patarin, *J. Am. Chem. Soc.*, 2001, **123**, 8129.
- 3 V. Eroshenko, R. C. Regis, M. Soulard and J. Patarin, *C. R. Phys.*, 2002, **3**, 111.
- 4 M. Soulard, J. Patarin, V. Eroshenko and R. Regis, *Stud. Surf. Sci. Catal.*, **2004**, *154B*, 1830.
- 5 N. Desbiens, I. Demachy, A. Fuchs, H. Kirsh-Rodeschini, M. Soulard and J. Patarin, *Angew. Chem., Int. Ed.*, 2005, **44**, 5310.
- 6 M. Trzpit, M. Soulard and J. Patarin, *Chem. Lett.*, 2007, **36**, 980.
- 7 M. Trzpit, M. Soulard, J. Patarin, N. Desbiens, F. Cailliez, A. Boutin, I. Demachy and A. Fuchs, *Langmuir*, 2007, **23**, 10131.
- 8 F. Cailliez, M. Trzpit, M. Soulard, I. Demachy, A. Boutin, J. Patarin and A. Fuchs, *Phys. Chem. Chem. Phys.*, 2008, **10**, 4817.
- 9 M. Trzpit, S. Rigolet, J.-L. Paillaud, C. Marichal, M. Soulard and J. Patarin, *J. Phys. Chem. B*, 2008, **112**, 7257.
- 10 M.-A. Saada, S. Rigolet, J.-L. Paillaud, N. Bats, M. Soulard and J. Patarin, *J. Phys. Chem. C*, 2010, **114**, 11650.
- 11 M.-A. Saada, M. Soulard, B. Marler, H. Gies and J. Patarin, *J. Phys. Chem. C*, 2011, **115**, 425.
- 12 L. Tzanis, M. Trzpit, M. Soulard and J. Patarin, *Microporous Mesoporous Mater.*, 2011, **146**, 119.
- 13 L. Tzanis, M. Trzpit, M. Soulard and J. Patarin, *J. Phys. Chem. C*, 2012, **116**, 4802.
- 14 L. Tzanis, B. Marler, H. Gies, M. Soulard and J. Patarin, *J. Phys. Chem. C*, 2013, **117**, 4098.
- 15 I. Khay, L. Tzanis, T. J. Daou, H. Nouali, A. Ryzhikov and J. Patarin, *Phys. Chem. Chem. Phys.*, 2013, **15**, 20320.
- 16 L. Tzanis, M. Trzpit, M. Soulard and J. Patarin, *J. Phys. Chem. C*, 2012, **116**, 20389.
- 17 A. Han, V. K. Punyamurtula and Y. Qiao, *Appl. Phys. Lett.*, 2008, **92**, 153117.
- 18 L. Tzanis, H. Nouali, T. J. Daou, M. Soulard and J. Patarin, *J. Mater. Lett.*, 2014, **115**, 229.
- 19 A. Han, W. Lu, T. Kim, Y. K. Punyamurtula and Y. Qiao, *Smart. Mater. Struct.*, 2009, **18**, 024005.
- 20 A. Han and Y. Qiao, *J. Mater. Res.*, 2007, **22**, 644.
- 21 A. Han, W. Lu, T. Kim, X. Chen and Y. Qiao, *Phys. Rev. E*, 2008, **78**, 031408.
- 22 I. Khay, T. J. Daou, H. Nouali, A. Ryzhikov, S. Rigolet and J. Patarin, *J. Phys. Chem. C*, 2014, **118**, 3935.
- 23 Handbook of surface and interface analysis, ed. J. C. Riviera and S. Myhra, Marcel Dekker, NY, 1998.
- 24 A. Burneau, J.-P. Gallas, in *The Surface Properties of Silicas*; Legrand, A. P., Ed.; John Wiley & Sons: Chichester, U.K., 1998, 145.
- 25 I. Persson, *Pure. Appl. Chem.*, 2010, **82**, 1901.
- 26 M. Mahler and I. Persson, *Inorg. Chem.*, 2012, **51**, 425.
- 27 D. H. Powell, A. C. Barnes, J. E. Enderby, G. W. Neilson and Ph. S. Salmon, *Farad. Discuss. Chem. Soc.*, 1988, **85**, 137.
- 28 D. W. Smith, *J. Chem. Educ.*, 1977, **54**, 540.
- 29 K. B. Yatsimirskii, *Theor. Exp. Chem.*, 1994, **30**, 1.

- 30 M. Camblor, A. Corma and S. Valencia, *Chem. Comm.*, 1996, **20**, 2365.
- 31 A. Boulitif and D. Louër, *J. Appl. Crystallogr.*, 1991, **24**, 987.
- 32 STOE WinXPOW, version 1.06; STOE and Cie: Darmstadt, Germany, 1999.